NPL Report RSA(EXT)40
March 1993

Measurement of the specific heat capacity of the electron-beam graphite calorimeter

A J Williams, D T Burns and M R McEwen
Division of Radiation Science and Acoustics
National Physical Laboratory
Teddington
Middlesex
United Kingdom
TW11 0LW

ABSTRACT

This report describes the design and construction of apparatus to measure the specific heat capacity of solid materials in the temperature range 18-32°C. The apparatus is designed to minimize heat losses from the sample in order to measure the specific heat to an accuracy of better than ±0.2% at the 95% confidence level. The results of a set of measurements on the graphite core of the electron-beam primary-standard radiation calorimeter are presented, along with a measurement of the effect of a large accumulated radiation dose on the specific heat of graphite.

ISSN 0955-9655

National Physical Laboratory
Teddington, Middlesex, UK, TW11 0LW

Approved on behalf of Chief Executive, NPL,
by Dr P Christmas, Head, Division of Radiation Science and Acoustics

CONTENTS

TABLES

FIGURES

1 INTRODUCTION

The Division of Radiation Science and Acoustics at the National Physical Laboratory is responsible for developing and maintaining the national standards in the UK for measurements of ionizing radiation. The practice of electron-beam radiotherapy in UK hospitals combined with the diminishing availability of ^{60}Co gamma-radiation sources for ion chamber calibrations necessitated the development of a primary-standard graphite calorimeter for use in electron-beams at radiotherapy dose levels and dose rates [1]. The estimated overall uncertainty in the measurement of graphite absorbed dose using the calorimeter is ±0.9% at the 95% confidence level; the largest single component of non-random uncertainty is in the measurement of the specific heat capacity of the graphite core of the calorimeter, estimated to be ±0.7%.

This report describes the apparatus used to measure specific heat capacity and the results of the measurements made on several samples of amorphous graphite. The results of a study of the effect of a large accumulated radiation dose on the specific heat are also included.

2 APPARATUS DESIGN AND CONSTRUCTION

2.1 OPERATING PRINCIPLES

The specific heat (capacity) of a material is defined in J kg^{-1} K^{-1} as

the thermal energy required (in joules) to raise the temperature of one kilogram of the material through one kelvin.

For graphite, this is expressed as

$$c_g = \frac{\textit{Energy input (J)}}{\textit{Mass (kg)} \times \textit{Temperature rise (K)}} = \frac{E}{m_g \Delta T} \qquad (1)$$

By using a measured amount of electrical energy E to induce a measured temperature change ΔT in a known mass of graphite m_g, the specific heat capacity of graphite can be calculated using this equation. Ideally, all of the electrical energy appears as heat in the graphite sample. However, it is known that heat will be lost from the system by a combination of radiative, conductive, and convective processes. Furthermore, it is not possible to construct the assembly without the use of materials other than the graphite sample. This means that impurity materials will be heated, so reducing the energy which is available to heat the graphite. By minimizing heat losses and impurity materials and calculating the residual effects, the specific heat capacity can be accurately measured.

2.2 DESIGN AND CONSTRUCTION OF APPARATUS

The apparatus is designed to thermally isolate the graphite sample from its surroundings, minimizing heat losses and reducing the effect of ambient temperature drifts. The mass of non-graphite impurity materials in direct contact with the graphite sample is kept to a minimum.

The graphite used for the measurements was from the same batch as is used in the primary-standard calorimeter. It is supplied by Southern Graphite, grade IG 11, with a density of 1.77 g cm^{-3}. Figure 1 shows a schematic diagram of a typical sample; it consists of a graphite cylinder 32.0 mm high by 33.5 mm in diameter with a mass of around 50 g. Two holes, each 1.6 mm in diameter by 4 mm deep, are drilled radially into the sample (at 90° to each other) to accommodate two 50 kΩ glass bead thermistors; one to sense temperature and one to heat the sample. Before the thermistors are inserted into the holes, each hole is filled with a zinc-oxide based heat-sink compound to improve the thermal contact between the thermistors and the graphite sample. After insertion of each thermistor, the excess heat-sink compound is *not* removed. By this means, the mass of the heat-sink compound is more easily calculated and so the impurity correction is better determined.

The wires from the heating thermistor are wrapped around the graphite cylinder 2½ times to reduce the amount of heat energy flowing directly out of the system by conduction along the wires. The wires are then glued to the cylinder using a small amount of cyanoacrylate adhesive; the adhesive is necessary because these wires are used to suspend the sample. The gauge of wire used is 44 swg (diameter 0.08 mm). The small cross-sectional area of this wire minimizes the heat lost by conduction along the wires (since the rate of heat loss is proportional to area × temperature gradient), while the ratio of the resistance of the wires to the thermistor resistance (0.022%) is not large enough to produce a significant correction due to energy dissipation in the wire.

The choice of the sample mass is a balance between minimizing time lags and temperature gradients within the sample, which favours a small mass, and the need for the temperature sensing and heating components to present a relatively small impurity, favouring a large mass. By experimentation, a mass of 50 g was chosen; the total impurity then represents a correction of less than 0.3%. The cylindrical shape of the sample is easy to machine; the diameter is very similar to the height in order to minimize the surface to volume ratio, which reduces heat losses.

Figure 2 shows the graphite jacket, vacuum system and temperature-controlled enclosure. The graphite sample is suspended within an aluminized graphite jacket of mass 7.2 kg and internal cylindrical dimensions 4.5 cm radius by 9 cm height; this assembly is placed within an evacuated bell-jar 30 cm in diameter by 35 cm high. The wires from the graphite heating and sensing thermistors exit the bell-jar through a rubber bung at the top. Aluminized mylar is fixed to the inside of the bell-jar and to the inside and outside surfaces of the graphite jacket; this serves to lower the surface emissivities of the jacket and bell-jar and hence reduce the amount of heat lost from the graphite sample to the surroundings by radiation.

The bell-jar is positioned directly on top of the vacuum pumping system which consists of a liquid-nitrogen cooled vapour lock, diffusion pump and two-stage rotary pump. The air pressure within the bell-jar is typically less than 10^{-6} mbar, making the contribution to heat loss by convection negligible. Surrounding the bell-jar is a temperature-controlled enclosure consisting of a 50×50×50 cm card box lined on the inside with 5 cm of foam rubber insulation. The air temperature inside the box is sensed at the top using a calibrated thermistor-bridge arrangement. The out-of-balance bridge voltage generated is amplified and used to power a series of wire-wound heating resistors placed around the base of the box; maximum power input is around 30 W. The air temperature may be set to any temperature between 18 and 32°C with a stability of better than ±50 mK.

3 TEMPERATURE AND ENERGY MEASUREMENTS

3.1 TEMPERATURE MEASUREMENTS

The temperature measuring assembly is based on that used for the electron-beam primary standard calorimeter [1], and is shown schematically in Figure 3. Briefly, it consists of a 50 kΩ glass bead thermistor (diameter 1½ mm) connected to a d.c. Wheatstone bridge constructed with precision wire-wound resistors and powered by a 1.2662 V precision voltage supply (long term stability ±6 ppm). The out-of-balance voltage from the bridge V_b is calibrated directly against a precisely-calibrated platinum resistance thermometer to give the bridge-voltage to temperature conversion function $T(V_b)$. Calibration details are given in Appendix A.

A digital voltmeter (DVM) with a precision of 6½ digits is used to measure the bridge voltage. Readings taken every 0.4 s are stored in the built-in memory file of the DVM. At the end of each measurement run the contents of the memory file are down-loaded via an IEEE-488 link to a controlling computer for storage on disc.

Using the calibration function $T(V_b)$, the computer calculates the graphite temperature directly from the stored bridge-voltage data. Figure 4 shows a typical temperature-time graph. Each data set is analysed to correct for the background temperature drift and heat losses during the heating period. Quadratic and linear least-squares fits to the pre- and post-heating data sets are extrapolated to the time corresponding to the mid-temperature of the heating period. The corrected temperature rise ΔT is taken as the difference between these extrapolated temperatures. For example, for the data in Figure 4 the pre-heat temperature drift is 0.11 mK/min, the post-heat drift is 0.21 mK/min and the corrected temperature rise is 16.386 mK.

The goodness of the corrected temperature rise can be estimated from a comparison of the measurements with a calculation of the expected heat losses by all of the dominant mechanisms. These calculations are summarized in Appendix A. The overall uncertainty in the measured value of ΔT is estimated to be ±0.12% at the 95% confidence level.

3.2 ELECTRICAL ENERGY INPUT

Figure 5 shows the apparatus for the electrical energy input. This consists of a constant voltage power supply V_S connected to a 2½ kΩ precision resistance R wired in series with a nominal 50 kΩ glass bead thermistor (of the same type as used for temperature sensor). The thermistor is embedded into a hole in the graphite sample using heat-sink compound and acts as a heating element. Power is switched on by a computer-controlled relay, the computer also measuring the duration t of the heating period. The calibration accuracy of the time measurement is discussed in Appendix B.

The voltage V_R generated across the series resistor R when the power is switched on is measured by a second DVM at a rate of approximately 400 readings per second, with up to 8000 readings being made in total over a period of 15-20 seconds. The calibration accuracy of the DVM when used in this mode is discussed in Appendix B. The voltage is repeatedly measured because the resistance of the heating thermistor varies over the heating period and therefore the power input also varies. Figure 6 shows the change in voltage across the series resistor with time for a typical run.

Measurement of the total energy input to the sample must correct for energy dissipated in the thin wires from the power supply to the heating thermistor. For a constant current I through the heating thermistor (i.e. a constant V_R)

$$\begin{aligned} \textit{Energy input to graphite} &= \textit{Energy input to system} - \textit{Energy lost in wires} \\ &= I V t - I^2 R_W t \end{aligned}$$

where V is the voltage across the heating thermistor (which is measured as V_S-V_R) and R_W is the resistance of the wires to the heating thermistor (including only those sections of the wires which are not included as an impurity). The current I through the heating thermistor is measured as V_R/R.

For a changing current equation 2 must be averaged over all N DVM readings;

$$E = \sum_{n=0}^{8000} \left[\frac{V_{R;n}}{R} (V_S - V_{R;n}) - \left(\frac{V_{R;n}}{R} \right)^2 R_W \right] \frac{t}{N}$$

where $V_{R;n}$ is the n^{th} reading of V_R. The magnitude of the correction for energy losses in the wires (i.e. the second term of equation 3) is typically (0.022±0.001)%, but varies with the heating rate.

Uncertainties in the energy measurements are discussed in Appendix B; the overall systematic uncertainty on the measured value of E is estimated to be ±0.06% at the 95% confidence level.

4 IMPURITY CORRECTION

The specific heat capacity of graphite was defined in equation 1. When the effect of those non-graphite components in good thermal contact with the sample are taken into account this becomes

$$c_g = \frac{E}{m_g \Delta T} \qquad \frac{\sum_i c_i m_i}{m_g} \tag{4}$$

where c_i is the specific heat capacity of the i^{th} non-graphite component and m_i is the mass of that component.

The best estimates of c_i and m_i for all impurity components are given in Table 1; the uncertainty arising from each component is derived from the uncertainties in c_i and m_i. Inserting the values for the total impurity and the uncertainties summed in quadrature into the second term in equation 4 gives

$$\frac{\sum_i c_i m_i}{m_g} = \frac{(84.7 \pm 7.2)\times 10^{-3}}{50\times 10^{-3}} = 1.69 \pm 0.15 \qquad J\ kg^{-1}K^{-1} \tag{5}$$

for a typical graphite sample of mass 50 g. This is a correction factor to the measured specific heat of approximately -0.24% with an uncertainty of only ±0.02% at the 95% confidence level.

Table 1 Correction for non-graphite components

Component	c_i J $kg^{-1}K^{-1}$	m_i $\times 10^{-3}$ kg	$c_i m_i$ $\times 10^{-3}$ J K^{-1}	Uncertainty $x10^{-3}$ J K^{-1}
copper wire	385	0.0302	11.6	0.8
thermistor glass × 2	780	0.0250	19.5	4.9
thermistor leads	385	0.0098	3.8	0.3
PTFE insulation	1000	0.0194	19.4	2.0
heat-sink compound	864	0.0236	20.4	4.1
adhesive	1000	0.0100	10.0	2.5
TOTAL	-	-	84.7	7.2

5 RESULTS

5.1 SPECIFIC HEAT CAPACITY OF GRAPHITE

Figure 7 shows a graph of the specific heat capacity of the graphite core of the primary-standard calorimeter as a function of temperature. The data consist of 66 measurements over the range 21-32°C which are fitted using a least-squares linear model. This fit gives

$$c_g = 644.9 + 2.94\,T \qquad J\ kg^{-1}K^{-1} \tag{6}$$

where T is the graphite temperature in Celsius. The rms deviation of the fitted equation from the mean result at each temperature is 0.02%.

The random uncertainty on the specific heat measurement is derived from the distribution of measurements for a given sample at a fixed temperature. A typical set of 11 measurements has a standard deviation of 0.05%. The best estimate of the random uncertainty at the 95% confidence level is ±0.03%.

This result agrees within 0.3% over the temperature range 20-30°C with the work of Richardson[2] at NPL who used a differential scanning calorimeter[3] to measure the specific heat of a number of samples of reactor grade graphite. Richardson states an overall uncertainty of ±1% at the 95% confidence level. The overall uncertainty on the present result is summarized in section 5.4.

5.2 SAMPLE TO SAMPLE VARIATIONS

Seven sets of measurements were made on four different samples of graphite (totalling over 300 measurements) over the temperature range 18-32°C. Three of the graphite samples were taken from the same batch of reactor grade graphite of density 1.81 g cm^{-3}; six sets of measurements were made on these samples. The fourth sample was taken from the graphite used for the primary-standard calorimeter (IG 11 grade supplied by Southern Graphite, density 1.77 g cm^{-3}); one extended set of measurements was made on this sample.

Samples which were measured on more than one occasion gave slightly different values for the specific heat capacity at 30°C on each occasion. Although small, these changes were larger than the random uncertainty on each measurement. It is evident that some unknown systematic error is changing each time the apparatus is assembled; perhaps the precise positioning of the sample is important. The best estimate of the uncertainty arising from this source, referred to as apparatus assembly, is ±0.08% at the 95% confidence level.

From all of the measurements taken together, it is not possible to distinguish the effect of the different graphite types from the assembly effect noted above. One can only deduce from this that the difference between the two graphite types is less than 0.1%.

5.3 DEPENDENCE ON ACCUMULATED RADIATION DOSE

In a separate experiment, the specific heat capacity of a particular graphite sample was measured to be (732.00 ± 0.10) J $kg^{-1}K^{-1}$ at 30°C (the uncertainty is the random component at the 95% confidence level). The sample was then removed from the apparatus and irradiated in a 10 MeV electron beam to a total dose in excess of 3 MGy (dosimetry based upon the primary-standard calorimeter). The specific heat was then re-measured in exactly the same way giving a result of (732.51 ± 0.09) J $kg^{-1}K^{-1}$. The measured change in the specific heat is +0.07%, which is typical of the change which is observed when an unirradiated sample is remeasured. Therefore within the uncertainties, no effect can be attributed to the radiation; the effect of a large accumulated dose on the specific heat capacity is considered to be negligible.

5.4 SUMMARY OF CORRECTION FACTORS AND UNCERTAINTIES

All correction factors and uncertainties are summarized in Table 2. The estimated overall uncertainty on the measurement of the specific heat of graphite at a given temperature is ±0.16% at the 95% confidence level.

6 ACKNOWLEDGEMENTS

The authors would like to thank I Stoker for his help with the computer programming, and also R Sanders and C Thomas for their help with the electronics.

Table 2 Summary of correction factors and uncertainties

Component	Correction (%)	Uncertainty (±% 95% c.l.)
random	-	0.03
temperature rise	-	0.12
energy input	-	0.06
losses in wires	-0.022	0.001
mass of graphite	-	0.002
impurity correction	-0.24	0.02
apparatus assembly	-	0.08
TOTAL	-0.26	0.16

APPENDICES

A TEMPERATURE CALIBRATION AND UNCERTAINTIES

A.1 THERMISTOR-BRIDGE CALIBRATION

The thermistor-bridge was calibrated as described by McEwen *et al*[4] (also summarized by Burns and Morris [1]). Briefly, the thermistor to be calibrated is placed in a graphite block together with a calibrated platinum resistance thermometer (PRT). The block is then immersed in a water bath. Under computer control, the temperature of the bath is varied in approximately 1 K steps over the range 18-35°C, each temperature step taking around an hour to achieve stability of ±10 mK. The bridge voltage and PRT resistance (from which the absolute temperature is derived) are measured at each temperature step. The temperature-voltage data, as shown in Figure 8, are fitted using a quartic model (close inspection of the residuals shows that a cubic model is insufficient). For the thermistor used in the specific heat measurements, the bridge-voltage to temperature conversion function is

$$T(V_b) = 26.129458 - 74.26875\,V_b + 15.8254\,V_b^2 - 68.296\,V_b^3 + 25.84\,V_b^4 \qquad (7)$$

where V_b is measured in volts and T is given in Celsius

The uncertainty in the PRT calibration is estimated to be ±0.1% at the 95% confidence level, while the uncertainty in the gradient of the thermistor calibration equation is estimated to be ±0.05%. The DVM which is used to read the bridge voltage is a calibrated 6½-digit device and does not contribute any significant uncertainty.

THEORETICAL ANALYSIS OF HEAT-LOSS MECHANISMS

Calculations were made at NPL [5] to estimate the amount of heat energy lost from the graphite sample by radiation, conduction and convection. Convection is easily shown to be negligible at the low air pressure achieved in the vacuum system. Similarly, simple models of the system are adequate to demonstrate that conduction along the heating and sensing wires is negligible, as is air conduction.

The only significant process of energy loss is thermal radiation, and this was kept to a minimum by enclosing the sample in an aluminized jacket with a high thermal inertia. By modelling this arrangement, it is possible to estimate the cooling gradient following a heating period; this compares well with the measured gradients. The calculations show that a quadratic extrapolation of the post-heating data result in an error of less than ±0.02%. The best estimate of the uncertainty in the correction for heat losses is taken to be ±0.03% at the 95% confidence level.

SUMMARY OF TEMPERATURE UNCERTAINTIES

The components contributing to the systematic uncertainty in the measurement of the temperature rise ΔT are summarized in Table 3. The overall uncertainty is estimated to be ±0.12% at the 95% confidence level.

Table 3 Uncertainties in measurement of the temperature rise

Component	95% c.l. (±%)
PRT calibration	0.10
thermistor calibration	0.05
radiative heat losses	0.03
QUADRATURE SUM	0.12

B ENERGY CALIBRATION AND UNCERTAINTIES

B.1 TIMER CALIBRATION

The internal clock of the controlling BBC computer is used to measure the duration of the heating period during a measurement run. The internal clock is calibrated against a NAMAS-calibrated timer. The timer is connected to the output of the computer-controlled relay and set to trigger on a 2 V edge, as shown in Figure 9. Measurements were made for 10, 15 and 20 s time intervals. The results of a typical calibration are shown in Table 4.

Table 4 Calibration of the computer clock

Set time (s)	10	15	20
Time as measured by NAMAS timer	10.0106	15.0116	20.0162
	10.0093	15.0118	20.0161
	10.0095	15.0111	20.0161
	10.0094	15.0113	20.0153
	10.0098	15.0114	20.0158
	10.0094	15.0117	20.0159
	10.0090	15.0113	20.0155
	10.0093	15.0118	20.0160
	10.0098	15.0116	20.0158
	10.0090	15.0114	20.0162
Mean t ± 95% c.l.	10.0095 ± 0.0005	15.0115 ± 0.0003	20.0159 ± 0.0003

The BBC clock underestimates the time by approximately 0.08%. This is taken into account in the computer analysis. The clock is re-calibrated regularly to correct for any long term drifts or systematic changes, for example due to modifications in the computer program which typically introduce 1-2 ms. The uncertainty in the calibrated timings is limited mainly by the variability of the triggering, which is estimated to be at the millisecond level. The uncertainty is therefore taken to be ±0.02% at the 95% confidence level. The absolute calibration uncertainty of the timer is negligible.

B.2 VOLTMETER CALIBRATION

The DVM which measures the voltage across the series resistor in the energy input circuit was calibrated to check that there was no change in reading when the DVM was used at 4½-digit resolution and triggering at 400 readings/s. A very stable reference voltage supply was used to provide a range of input voltages to the DVM, typical of the voltages normally measured. For each input voltage, 1000 readings were taken at a resolution of 4½ digits and a rate of 400 readings/s. The results of eight such measurements are shown in Table 5.

Table 5 Calibration of the DVM at 400 readings/s

Reference voltage	Mean DVM reading	95% c.l. (±%)	Correction (%)
2.200043	2.200967	0.012	-0.042
2.400041	2.400462	0.012	-0.018
2.600050	2.600076	0.013	-0.001
2.800048	2.799688	0.013	+0.013
3.000054	3.000081	0.012	-0.001
3.200053	3.200625	0.015	-0.018
3.400058	3.400495	0.014	-0.013
3.600063	3.600373	0.014	-0.009

The correction factor is generally less than the 95% uncertainty on the result. Therefore no correction is applied to the measurements and an uncertainty of ±0.02% is attributed to the use of the DVM in this mode. The absolute calibration uncertainty of the DVM is negligible.

B.3 DEPENDENCE ON POWER LEVEL AND HEATING PERIOD

As an additional check that heat losses are small and adequately accounted for in the data analysis, the specific heat capacity was measured for a series of different power input levels and heating periods to investigate any possible systematic effects. The results are shown in Tables 6 and 7.

Table 6 Effect of power level on specific heat measurement

Rate of energy input (mW)	Specific heat capacity at 25°C ($J\ kg^{-1}K^{-1}$)	95% c.l. ($J\ kg^{-1}K^{-1}$)
33	718.26	0.25
61	718.19	0.46
105	718.10	0.16

For the power-level measurements summarized in Table 6, the results at different power levels all fall within the 95% confidence limits. Even if a trend is assumed, the best estimate at zero power level is around 718.4 J $kg^{-1}K^{-1}$, compared to 718.2 J $kg^{-1}K^{-1}$ at the more usual power level close to 50 mW. This is a correction of at most +0.03%. No correction is made; instead, an uncertainty of ±0.04% is included.

Table 7 Effect of heating period on specific heat measurement

Heating period (s)	Specific heat capacity at 30°C (J $kg^{-1}K^{-1}$)	95% c.l. (J $kg^{-1}K^{-1}$)
10.0095	731.39	0.12
15.0115	731.50	0.27
20.0138	731.34	0.15

For the heating-period measurements summarized in Table 7, the results again fall within the 95% confidence limits, and no trend can be determined. No correction is made, and an uncertainty of ±0.03% is included.

B.4 SUMMARY OF ENERGY UNCERTAINTIES

The components contributing to the systematic uncertainty in the measurement of the energy input E are summarized in Table 8 (energy loss in the heating wires is treated separately in section 3.2).

Table 8 Uncertainties in the measurement of the energy input

Component	95% c.l. (±%)
time measurements	0.02
fast-read DVM	0.02
power level	0.04
heating period	0.03
series resistor	0.003
digitisation	0.02
QUADRATURE SUM	0.06

A small component is included for the measurement of the 2.5 kΩ series resistor R using a calibrated resistance meter. An additional component is included for the digitisation of the voltage measurement into 5000 or more bins; ±1 bin represents ±0.02%. The overall uncertainty is estimated to be ±0.06% at the 95% confidence level.

REFERENCES

1 D T BURNS and W T MORRIS, *A graphite calorimeter for electron beam dosimetry*, Proceedings of International Atomic Energy Agency symposium 'High Dose Dosimetry for Radiation Processing' (IAEA, Vienna, 1991), p123.

2. M J RICHARDSON, private communication (National Physical Laboratory, Teddington, 1990).

3. M J RICHARDSON, Chapter 18 in *Compendium of Thermophysical Property Measurement Methods Volume 1: Recommended Measurement Techniques and Practices,* edited by K D Maglić, A Cezairliyan and V E Peletsky (Plenum Press, New York, 1992).

4. M R McEWEN, D T BURNS and A J WILLIAMS, *The use of thermistors in the NPL electron-beam calorimeter*, NPL Report RSA(EXT)41 (National Physical Laboratory, Teddington, 1993).

5. D R SHIPLEY, S DUANE and A R DUSAUTOY, *Heat loss mechanisms in a measurement of specific heat capacity of graphite*, NPL Report RSA(EXT) to be published (National Physical Laboratory, Teddington, 1993).

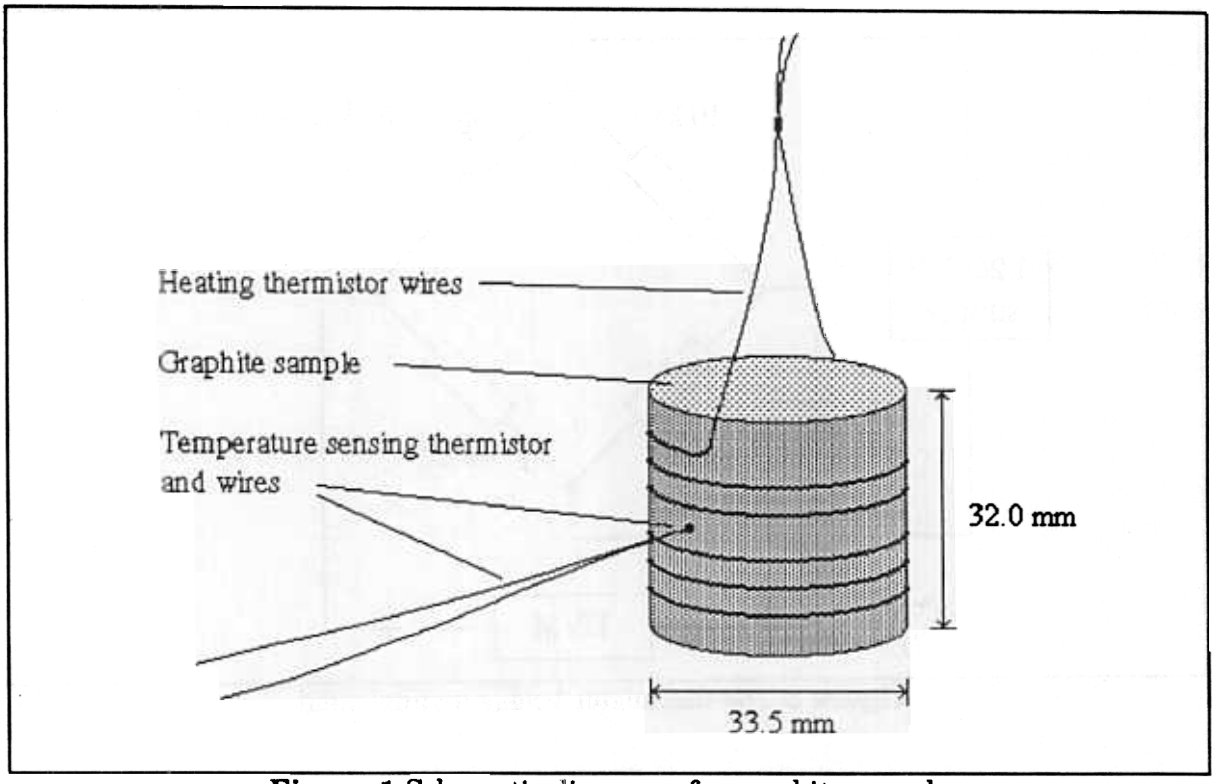

Figure 1 Schematic diagram of a graphite sample

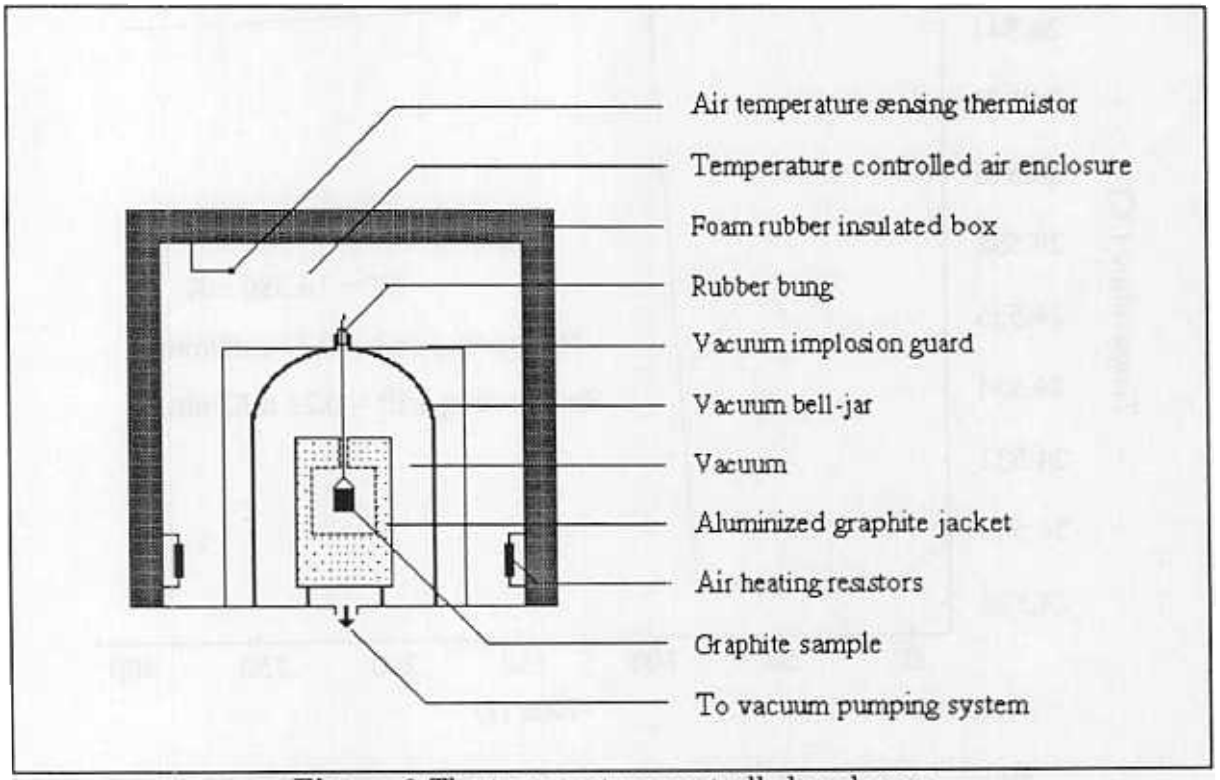

Figure 2 The temperature-controlled enclosure

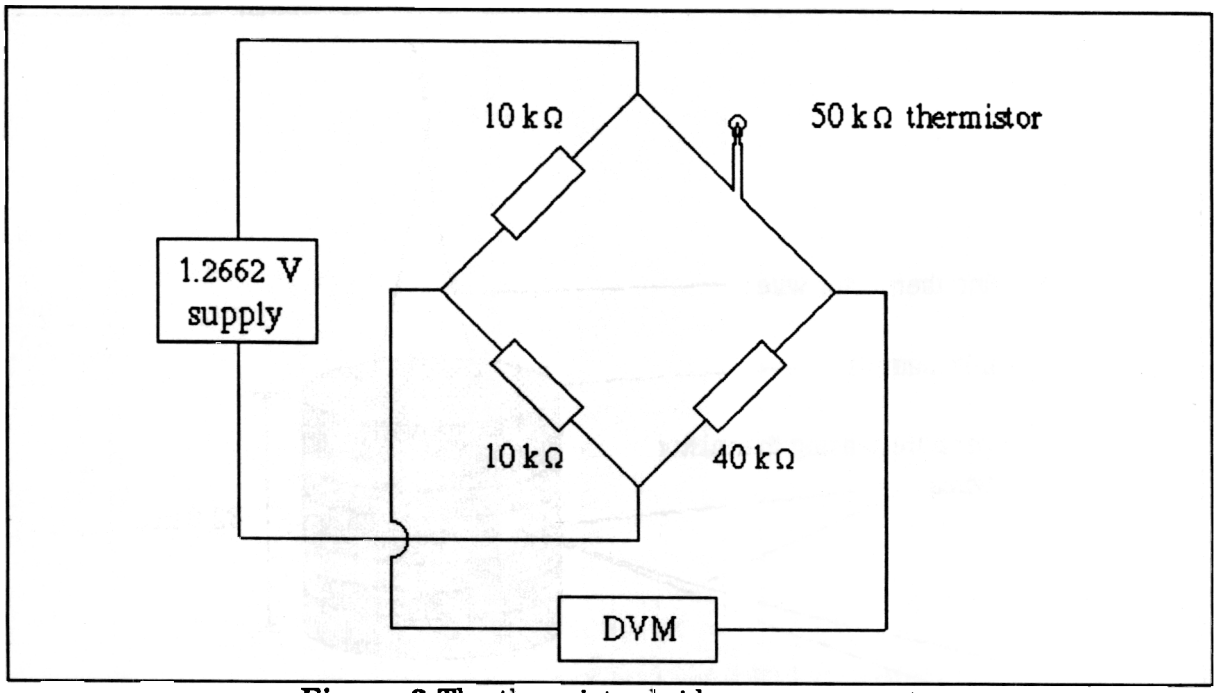

Figure 3 The thermistor bridge arrangement

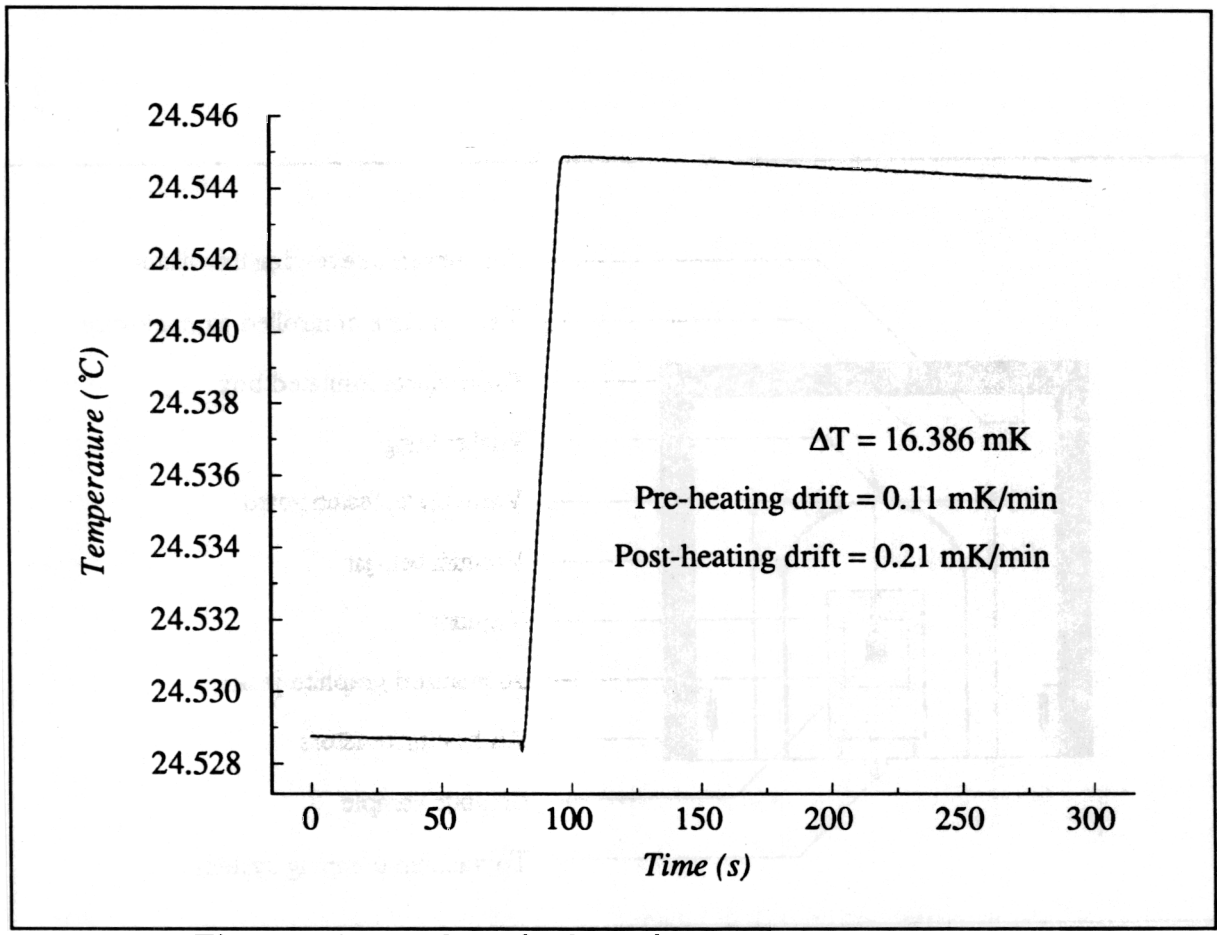

Figure 4 A typical graph of sample temperature against time

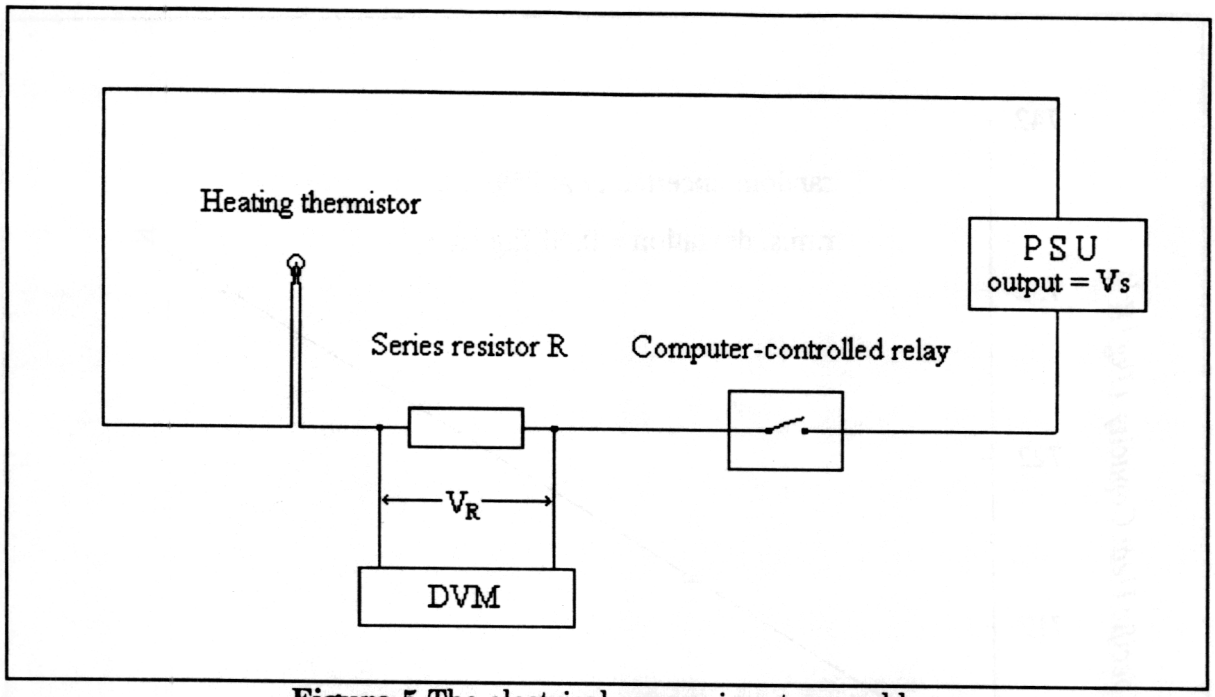

Figure 5 The electrical energy input assembly

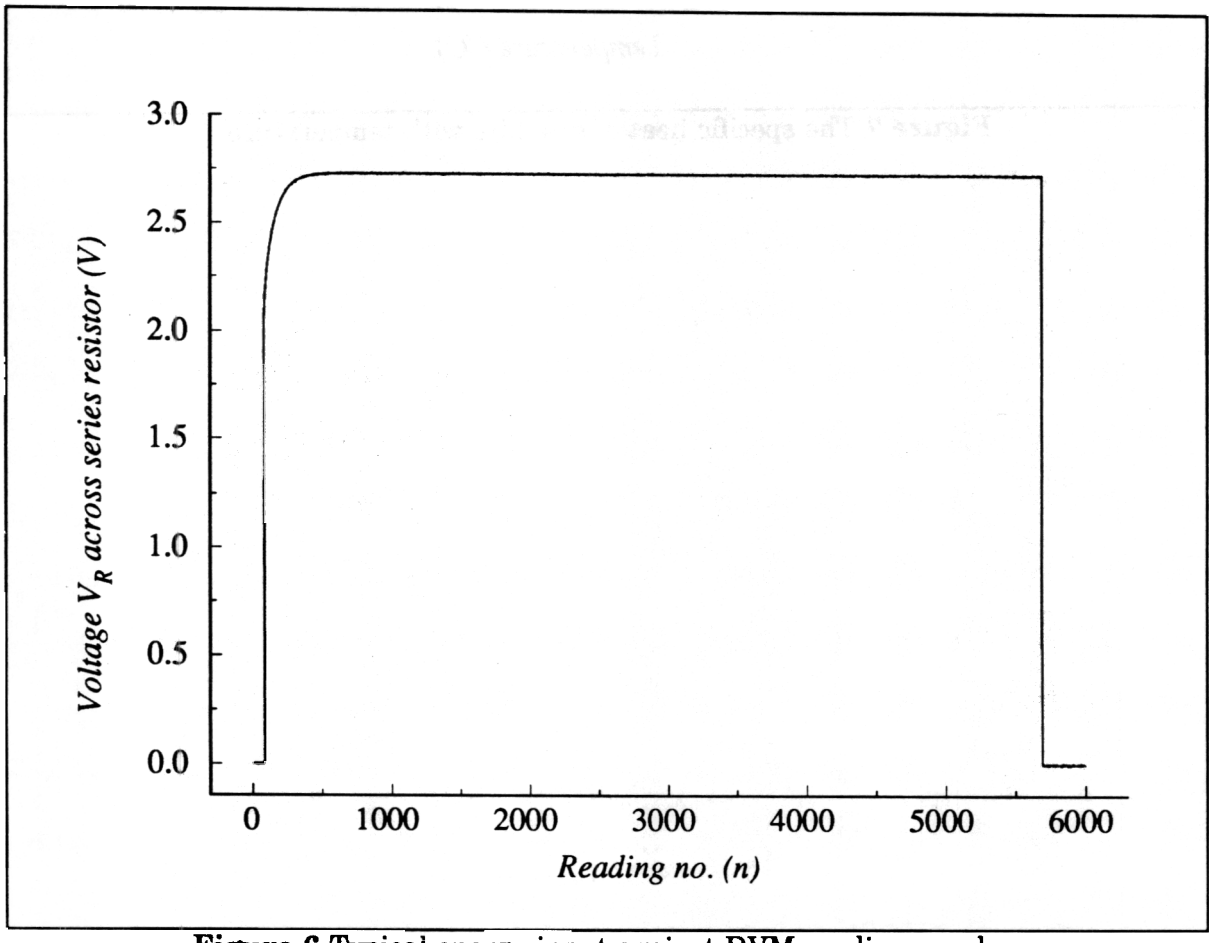

Figure 6 Typical energy input against DVM reading number

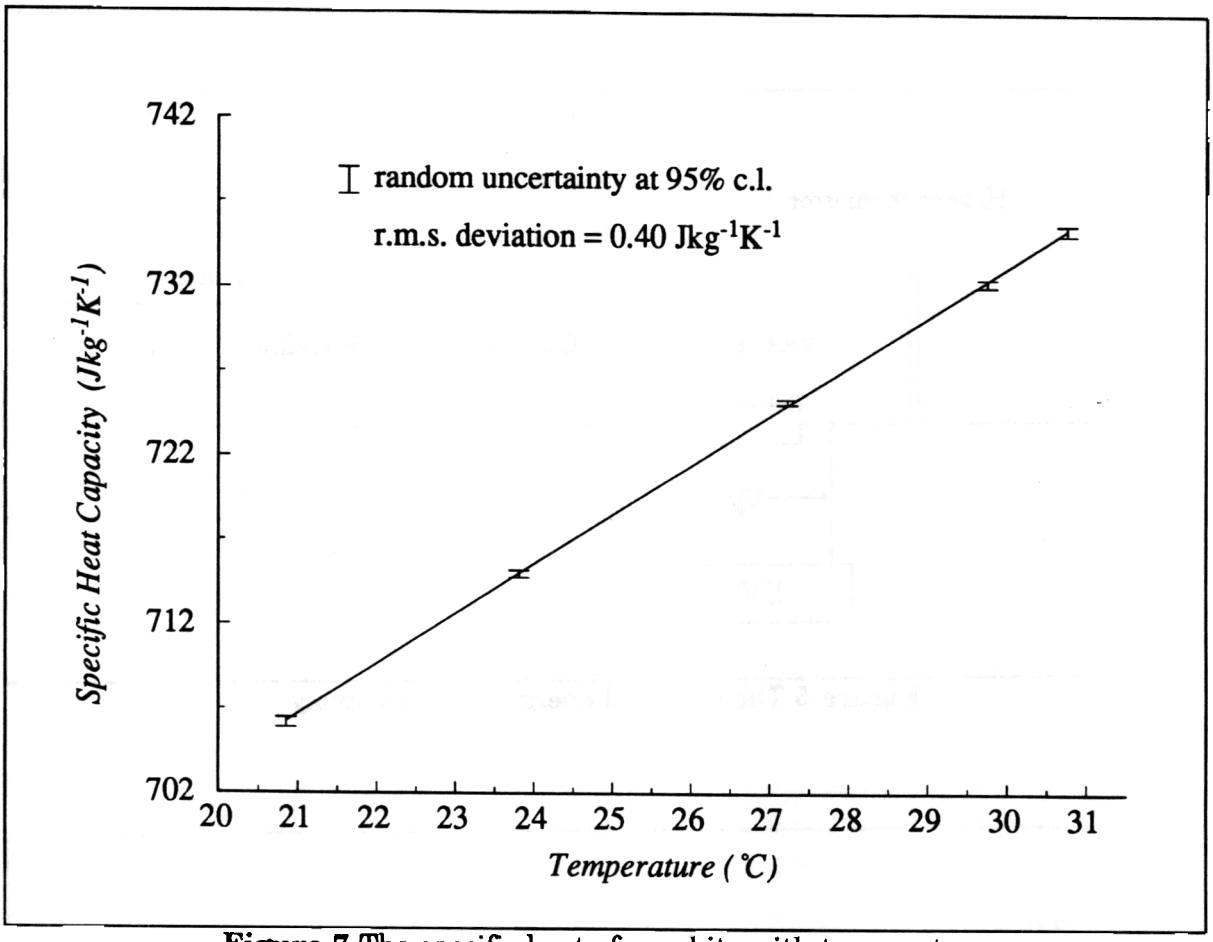

Figure 7 The specific heat of graphite with temperature

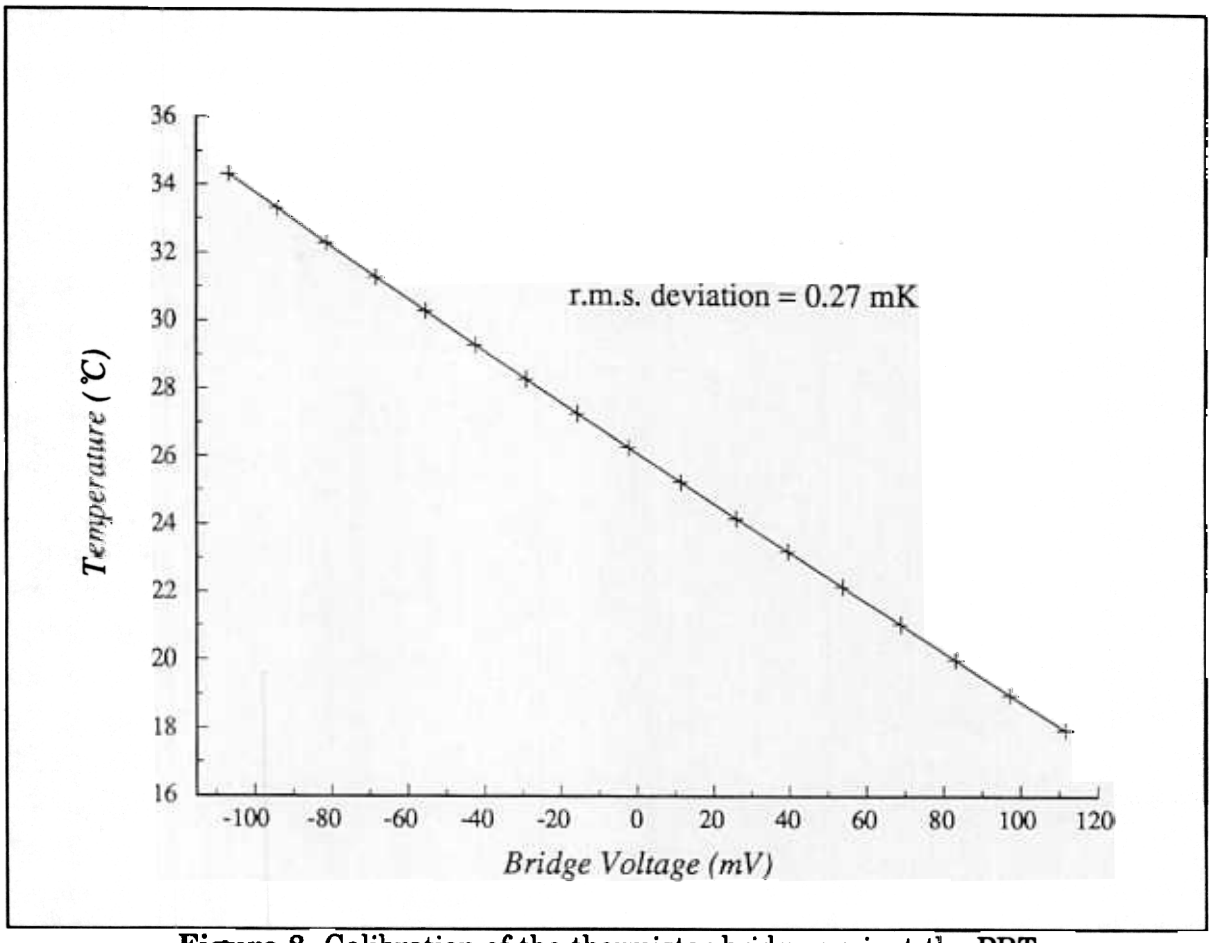

Figure 8 Calibration of the thermistor bridge against the PRT

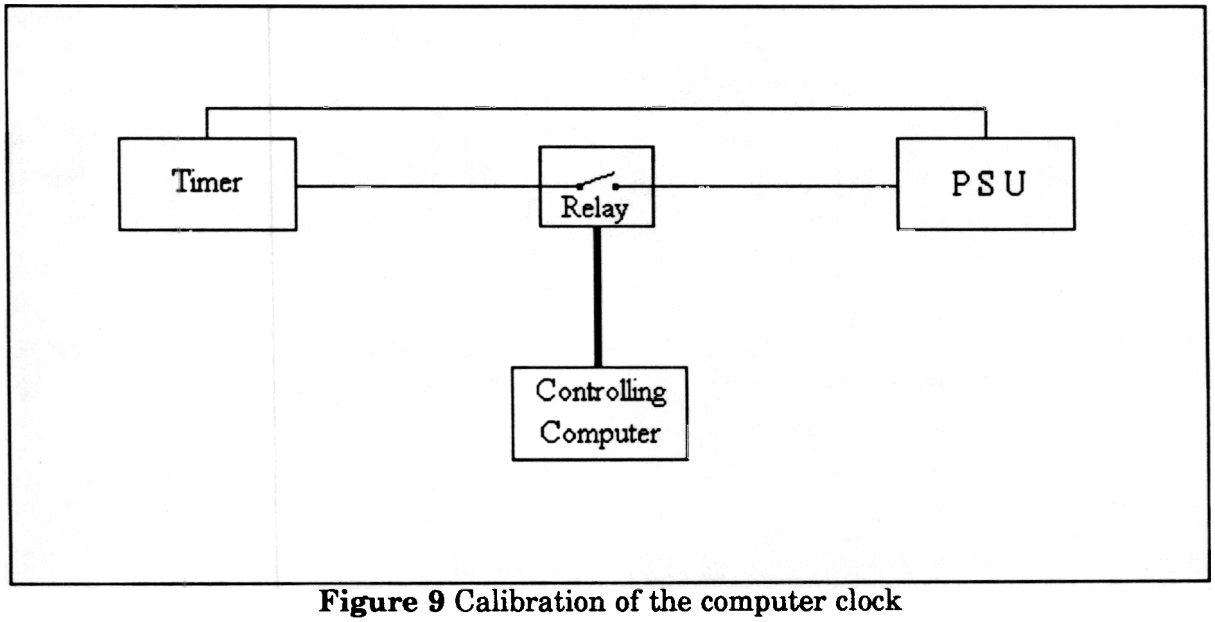

Figure 9 Calibration of the computer clock